DOI: 10.24996/ijs.2025.66.11.31

ISSN: 0067-2904

Impact of Porous Media and Magnetic Field on Peristaltic Transport of a Second-Grade Dusty Fluid Through a Symmetric Channel

Fatima K. Addullah*, Ahmed M. Abdulhadi
Department of Mathematics, College of Science, University of Baghdad, Baghdad, Iraq

Received: 20/5/2024 Accepted: 3/11/2024 Published: 30/11/2025

Abstract:
In this research, we studied the effect of porous media, magnetic field, and heat transfer on the peristaltic flow of a second-order dusty fluid in a symmetrical cylindrical channel. The coupled nonlinear differential equations, which represent the motion of dust and fluid molecules, are formulated. These equations are solved by using the perturbation method with the help of the mathematics package; we obtained an approximate analytic solution. The impact of different kinds of parameters, like the Prandtl number, Renold number, wave number, second-grade parameter, Hartman number, wave length, permeability of the medium, and Darcy number, is discussed on the fluid velocity, fluid temperature, flow pattern, dust particle flow pattern, and pressure. The results show that increasing the permeability of the porous medium has a negligible effect on the size and number of boluses, with the bolus size decreasing by a small percentage as the Darcy number increases. We observed that the number of boluses decreases and their size increases as the Hartman number increases. Finally, we discussed the results graphically using MATHMETICA software.

Keyword: Peristaltic transport, heat transfer. Magnetic field, porous media, second-grade dusty fluid

تأثير الوسط المسامي والحقل المغناطيسي على جريان تمعجي لمائع مغبر من الدرجة الثانية في قناة اسطوانية متناظرة

فاطمة كميت.عبدالله* , احمد مولود عبدالهادي
قسم الرياضيات, كلية العلوم, جامعة بغداد, بغداد, العراق

الخلاصة:
درسنا في هذا البحث تأثير الوسط المسامي والمجال المغناطيسي وانتقال الحرارة على الجريان التمعجي لمائع مغبر من الدرجة الثانية في قناة أسطوانية متناظرة. تمت صياغة المعادلات التفاضلية غير الخطية المقترنة، والتي تمثل حركة جزيئات الغبار والسوائل. يتم حل هذه المعادلات باستخدام طريقة الاضطراب بمساعدة الحزمة الرياضية؛ حصلنا على حل تحليلي تقريبي. تمت مناقشة تأثير أنواع مختلفة من المعلمات، مثل رقم براندتل، ورقم رينولد، ورقم الموجة، ومعلمة الدرجة الثانية، ورقم هارتمان، وطول الموجة، ونفاذية الوسط، ورقم دارسي، على سرعة المائع ودرجة حرارته ونمط تدفق جسيمات الغبار ، والضغط. أظهرت النتائج أن زيادة نفاذية الوسط المسامي له تأثير ضئيل على حجم وعدد البلعات، حيث يتناقص حجم البلعة بنسبة

*Email: f.abdullah@coeng.uobaghdad.edu.iq

مئوية صغيرة مع زيادة رقم دارسي. لاحظنا أن عدد البلعات يتناقص ويزداد حجمها مع زيادة عدد هارتمان.
وأخيرا، ناقشنا النتائج بيانيا باستخدام برنامج MATHMATACA.

Introduction

Flow is created when a wave moves along the walls of a flexible tube. This progressive wave motion is known as peristalsis. The phenomenon of peristalsis in an elastic tube is especially used by a number of biological systems, such as the cardiovascular system, the trachea, the duodenum, and the fallopian tube of females. Fluids become hazy and exhibit very complex dynamics when they contain differently distributed solid molecules in colloidal suspension. Unrefined petroleum, crude oils, human urine with stones or glucose particle suspension, and a variety of meals with pulpy granules are a few examples of these dusty liquids. Researchers have conducted studies on the peristaltic transfer of various fluids [1-9]. In the extrusion procedures for plastic and metal, stretching cylinders are essential. A stretched cylinder was used to study the Darcy Forchheimer flow of a tri-hybrid nanofluid based on water and carboxymethyl cellulose (CMC) [10]. The idea of using peristaltic pumping mechanics in second order a non-Newtonian fluid through an axisymmetric conduit were given by [11]. In 2018, variable viscosity of MHD second-grade fluid toward a stretching sheet with variable thickness was studied [12]. The behavior of second-grade dusty fluid flowing through a flexible tube whose walls are induced by the peristaltic movement was investigated [13]. The related studies of non-Newtonian fluids focus in determining the feasibility of physiology and engineering practical applications [14-21]. Where the results established that heat, transfer is significant in the geophysical sciences and engineering applications. Thus, the applications based on subterranean energy transit in geothermal reservoirs include thermal insulation, drying of porous substances, enhanced recovery of oils and fossil fuels, catalytic reactors with packed beds, and cooling of nuclear reactors [19]. The peristaltic motion of a dusty fluid flowing through a channel determined the amount of heat transfer [22]. In [23], demonstrated the effects of velocity slip on magnetohydrodynamic (MHD) peristaltic fluid transport through a porous medium in the presence of mass and heat transfers. However, [24] demonstrated the importance of the impact of a revolving medium with flexible walls on the peristaltic transport of the MHD fluid. Researchers investigated the natural convection of power-law fluids over a horizontal, flat plate with a constant heat flux. above a level, horizontal plate experiencing a steady heat flux [25]. Researchers examined mass and heat transfer as well as the peristaltic transport characteristics of a Johnson Segelman fluid travelling through an irregularly curved conduit [26]. Researchers used a new computational fluid dynamics approach to simulate the processes of sloshing and evaporation in a cryogenic fuel tank [27]. Using a simulation of the dynamics of multifactorial fluids, researchers examined a tank for village storage compressed on cylinders [28]. Consideration was given to a second-grade dusty fluid flowing in a flexible tube with walls created by peristaltic movement in order to comprehend the transport process in the presence of heat transfer [16]. The aim of this paper is to investigate the effect of porous media and magnetic field to the peristatic transport of a second-grade dusty fluid flown with heat transfer through a symmetric channel.

2. Mathematical model

It was considered that small, even-sized solid molecules with a number density (N) were streaming in two dimensions in an axially symmetric manner through a conduit. The solid molecules have constant densities. Long wavelength peristaltic waves are further considered to be able to propagate along the channel walls. See Figure (1).

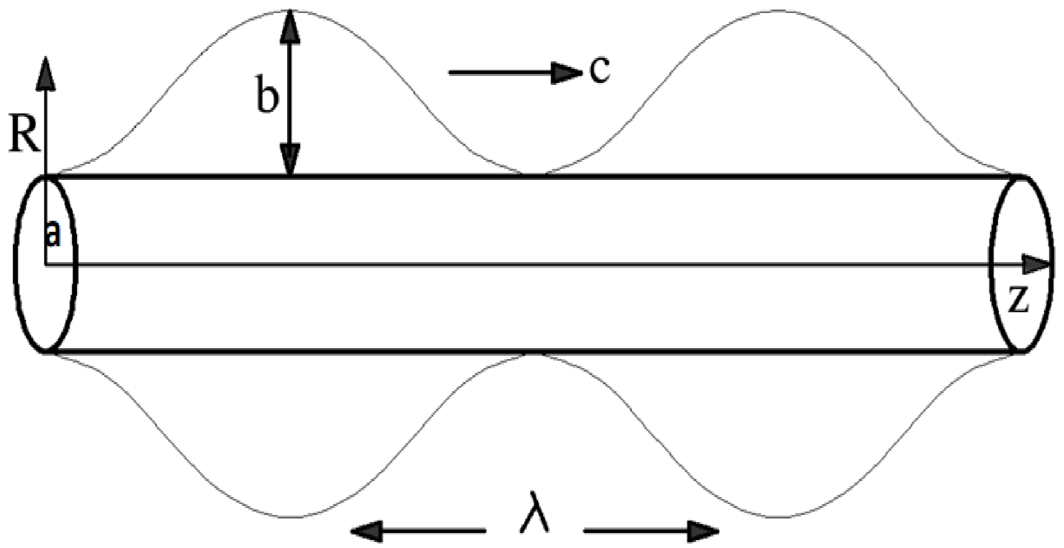

Figure .1: Geometry graph of the problem

Let $(R\ ,Z,t)$ to be the cylindrical coordinate system defined by R the along the radial, Z the axial direction, and *t* is the time. The sketch diagram of the cylindrical wall is [16] :

$$\bar{h}(\bar{z},\bar{t}) = a + b\, sin\frac{2\pi}{\lambda}(\bar{z} - c\bar{t}), \tag{1}$$

where a is the radius of the tube, b the wave amplitude, c the speed of propagating wave, finally λ wavelength.

Can be written the stress tensor (constitutive relation) of the second-grade dusty fluid as [29]:

$$\bar{S} = -\bar{P}I + \bar{\tau}. \tag{2}$$

Here, $\bar{P}$ represents the pressure, I is the identity tensor and $\bar{\tau}$ is the extra stress tensor given by:

$$\bar{\tau} = \mu A_1 + \alpha_1 A_2 + \alpha_2 A_1^2. \tag{3}$$

Where μ is the dynamic viscosity α_1 an α_2 are the material, constant, $\mu > 0, \alpha_1, \alpha_2 > 0$, the kinematic tensors A_1 and A_2 can be written as [30]:

$$A_1 = \left(grad\vec{V}\right) + (grad\vec{V})^T. \tag{4}$$

$$A_2 = \frac{dA_1}{dt} + A_1.\left(grad\vec{V}\right) + \left(grad\vec{V}\right)^T.A_1. \tag{5}$$

Where $grad\vec{V}$ is the fluid velocity gradient in the polar coordinate and $(grad\vec{V})^T$ is the transpose of the fluid velocity gradient in the polar coordinate $(\bar{R}, 0.\bar{Z})$, [28].

$$grad\vec{V} = \begin{bmatrix} \frac{\partial\bar{U}}{\partial\bar{R}} & \frac{1}{\bar{R}}\frac{\partial\bar{U}}{\partial\emptyset} - \frac{\bar{V}}{\bar{R}} & \frac{\partial\bar{U}}{\partial\bar{Z}} \\ \frac{\partial\bar{V}}{\partial\bar{R}} & \frac{1}{\bar{R}}\frac{\partial\bar{V}}{\partial\emptyset} + \frac{\bar{U}}{\bar{R}} & \frac{\partial\bar{V}}{\partial\bar{Z}} \\ \frac{\partial\bar{W}}{\partial\bar{R}} & \frac{1}{\bar{R}}\frac{\partial\bar{W}}{\partial\emptyset} & \frac{\partial\bar{W}}{\partial\bar{Z}} \end{bmatrix}. \tag{6}$$

3. Governing equations

The equation of motion for steady flow in incompressible stress of an asymmetric of the magnetic field via porous media in the fixed frame $(\bar{R}, \bar{Z})$ is:

$$\rho\left[\bar{U}\frac{\partial\bar{U}}{\partial\bar{R}}+\bar{W}\frac{\partial\bar{U}}{\partial\bar{Z}}\right]=-\frac{\partial\bar{P}}{\partial\bar{R}}+\frac{1}{\bar{R}}\frac{\partial}{\partial\bar{R}}(\bar{R}\bar{\tau}_{rr})+\frac{\partial}{\partial\bar{Z}}\bar{\tau}_{rz}-\frac{\bar{\tau}_{\theta\theta}}{\bar{R}}+KN(\bar{u}_s-\bar{u})-\frac{\mu}{\bar{K}}(\bar{u}_s-\bar{u})-\sigma B_\circ{}^2(\bar{u}_s-\bar{u}). \quad (7)$$

$$\rho\left[\bar{U}\frac{\partial\bar{W}}{\partial\bar{R}}+\bar{W}\frac{\partial\bar{W}}{\partial\bar{Z}}\right]=-\frac{\partial\bar{P}}{\partial\bar{Z}}+\frac{1}{\bar{R}}\frac{\partial}{\partial\bar{R}}(\bar{R}\bar{\tau}_{rz})+\frac{\partial}{\partial\bar{Z}}\bar{\tau}_{zz}+KN(\bar{W}_s-\bar{W})-\rho g\alpha(\bar{T}-\bar{T}_\circ). \quad (8)$$

Also, the equations of solid molecules motion, and heat transfer are defined by

$$\bar{U}_s+\frac{\partial\bar{U}_s}{\partial\bar{R}}+\bar{W}_s\frac{\partial\bar{U}_s}{\partial\bar{Z}}=\frac{K}{m}(\bar{U}-\bar{U}_s). \quad (9)$$

$$\bar{U}_s+\frac{\partial\bar{W}_s}{\partial\bar{R}}+\bar{W}_s\frac{\partial\bar{W}_s}{\partial\bar{Z}}=\frac{K}{m}(\bar{W}-\bar{W}_s). \quad (10)$$

$$\rho c_p\left[\bar{U}\frac{\partial\bar{T}}{\partial\bar{R}}+\bar{W}\frac{\partial\bar{T}}{\partial\bar{Z}}\right]=k\left[\bar{U}\frac{\partial^2\bar{T}}{\partial\bar{R}^2}+\frac{1}{\bar{R}}\frac{\partial\bar{T}}{\partial\bar{R}}+\frac{\partial^2\bar{T}}{\partial\bar{Z}^2}\right]+Q_\circ. \quad (11)$$

There is unsteady flow between the two tubes at the fixed coordinates $(\bar{R}, \bar{Z})$. When a wave frame $(\bar{r}, \bar{z})$ travels at the same speed as the wave in the Z direction, it becomes steady. The changes:

$$\bar{r}=\bar{R},\ \bar{z}=\bar{Z}-c\bar{t},\ \bar{u}=\bar{U},\ \bar{w}=\bar{W}-c,\ \bar{w}_s=\bar{W}_s-c,\ \bar{u}_s=\bar{U}_s. \quad (12)$$

The flow of Equations (7) - (11) are given by:

$$\rho[\bar{u}\frac{\partial\bar{u}}{\partial\bar{r}}+(\bar{w}+c)\frac{\partial\bar{u}}{\partial\bar{z}}]=-\frac{\partial\bar{p}}{\partial\bar{r}}+\frac{1}{\bar{r}}\frac{\partial}{\partial\bar{r}}(\bar{r}\bar{\tau}_{rr})+\frac{\partial}{\partial\bar{z}}\bar{\tau}_{rz}-\frac{\bar{\tau}_{\theta\theta}}{\bar{r}}+KN(\bar{u}_s-\bar{u})-\frac{\mu}{\bar{K}}(\bar{u}_s-\bar{u})-\delta\beta_\circ{}^2(\bar{u}_s-\bar{u}). \quad (13)$$

$$\rho\left[\bar{u}\frac{\partial\bar{w}}{\partial\bar{r}}+(\bar{w}+c)\frac{\partial\bar{w}}{\partial\bar{z}}\right]=\frac{\partial\bar{p}}{\partial\bar{z}}+\frac{1}{\bar{r}}\frac{\partial}{\partial r}(\bar{r}\bar{\tau}_{rz})+\frac{\partial}{\partial z}\bar{\tau}_{zz}+KN(\bar{w}_s-\bar{w})-\rho g\alpha(T-T_\circ). \quad (14)$$

And

$$\bar{u}_s\frac{\partial\bar{u}_s}{\partial\bar{r}}+(\bar{w}+c)\frac{\partial\bar{u}_s}{\partial\bar{z}}=\frac{K}{m}(\bar{u}-\bar{u}_s). \quad (15)$$

$$\bar{u}_s\frac{\partial\bar{w}_s}{\partial\bar{r}}+(\bar{w}+c)\frac{\partial\bar{w}_s}{\partial\bar{z}}=\frac{K}{m}(\bar{w}-\bar{w}_s). \quad (16)$$

$$\rho c_p\left[\bar{u}\frac{\partial T}{\partial\bar{r}}+(\bar{w}+c)\frac{\partial\bar{T}}{\partial\bar{z}}\right]=k\left[\frac{\partial^2\bar{T}}{\partial\bar{r}^2}+\frac{1}{\bar{r}}\frac{\partial\bar{T}}{\partial\bar{r}}+\frac{\partial^2\bar{T}}{\partial\bar{z}^2}\right]+Q_\circ. \quad (17)$$

4. Dimensionless parameters

The following dimensionless variables and parameters are introduced:

$$\left.\begin{array}{l}\theta=\frac{\bar{T}-\bar{T}_\circ}{\Delta\bar{T}},\delta=\frac{a}{\lambda},h=\frac{\bar{h}}{a},Re=\frac{\rho ca}{\mu},Pr=\frac{\mu c_p}{k},Gr=\frac{\rho g\alpha\Delta Ta^2}{\mu c},\\ \beta=\frac{Q_\circ a^2}{k\Delta T},\alpha_1=\frac{\alpha_1 c}{\mu a},A=\frac{KNa^2}{\mu},B=\frac{Ka}{mc},\phi=\frac{b}{a},\ \frac{1}{Da}=\frac{a^2}{\tilde{K}},\\ H=\sqrt{\frac{\delta}{\mu}}B_\circ a,\ \nabla^2=\frac{\partial^2}{\partial r^2}+\frac{1}{r}\frac{\partial}{\partial r}+\delta^2\frac{\partial^2}{\partial z^2}\end{array}\right\}. \quad (18)$$

Where $\theta, \delta, Re, Pr, Gr, \beta, \alpha_1, a, b, c, \rho, \mu, k, K, \alpha, H, \lambda, \widetilde{K}$ and Da are the temperature distribution, wave number, Renold number, Prandtl number, Grashoff number, sink parameter, second - grade parameter, channel radius, wave amplitude, wave speed, density of fluid, viscosity coefficient, thermal conductivity, stokes resistance coefficient, thermal expansion coefficient, Hartman number, wave length, permeability of the medium and Darcy number, respectively.

According to Equation (1), the dimensionless shape of the peristaltic channel walls is in $h(z)$

$$h(z)=1+\phi\sin(z). \quad (19)$$

By using the dimensionless expressions given in (18) of Equations (13)-(17) becomes:

$$\delta^3 Re\left[u\frac{\partial u}{\partial r}+(w+1)\frac{\partial u}{\partial z}\right]=-\frac{\partial p}{\partial r}+\frac{\delta}{r}\frac{\partial}{\partial r}(r\tau_{rr})+\delta^2\frac{\partial}{\partial z}(\tau_{rz})-\frac{\delta}{r}\tau_{\theta\theta}+\delta^2 A(u_s-u)-\delta^2\frac{1}{Da}(u_s-u)-\delta^2 H^2(u_s-u). \quad (20)$$

$$\delta Re\left[u\frac{\partial w}{\partial r}+(w+1)\frac{\partial w}{\partial z}\right]=-\frac{\partial p}{\partial z}+\frac{1}{r}\frac{\partial}{\partial r}(r\tau_{rz})+\delta\frac{\partial}{\partial z}\tau_{zz}+A(w_s-w)-Gr\,\theta. \quad (21)$$

$$\delta(u_s\frac{\partial u_s}{\partial r}+(w_s+1)\frac{\partial u_s}{\partial z})=B(u-u_s). \quad (22)$$

$$\delta\left[u_s\frac{\partial w_s}{\partial r}+(w_s+1)\frac{\partial w_s}{\partial z}\right]=B(w-w_s). \quad (23)$$

$$\delta\, Re\, Pr\left[u\frac{\partial\theta}{\partial r}+(w+1)\frac{\partial\theta}{\partial z}\right]=\nabla^2\theta+\beta. \quad (24)$$

By using the dimensionless expressions given in (18) of stress tensor becomes:

$$\tau_{rr}=2\delta\frac{\partial u}{\partial r}+\alpha_1\left[\left(\frac{\partial w}{\partial r}\right)^2-\delta^4\left(\frac{\partial u}{\partial z}\right)^2+2\delta^2\left(u\frac{\partial^2 u}{\partial r^2}+w\frac{\partial^2 u}{\partial r\partial z}\right)\right]. \quad (25)$$

$$\tau_{rz}=\delta^2\frac{\partial u}{\partial z}+\frac{\partial w}{\partial r}+\alpha_1\left[\delta^3\frac{\partial u}{\partial r}\frac{\partial u}{\partial z}+\delta\frac{\partial w}{\partial r}\frac{\partial w}{\partial z}-\delta\frac{\partial u}{\partial r}\frac{\partial w}{\partial r}-\delta^3\frac{\partial u}{\partial z}\frac{\partial w}{\partial z}+\delta^3 u\frac{\partial^2 u}{\partial r\partial z}+\delta u\frac{\partial^2 w}{\partial r^2}+\delta^3 w\frac{\partial^2 u}{\partial z^2}+\delta w\frac{\partial^2 w}{\partial r\partial z}\right]. \quad (26)$$

$$\tau_{zz}=2\delta\frac{\partial w}{\partial z}+\alpha_1\left[\delta^4\left(\frac{\partial u}{\partial z}\right)^2-\left(\frac{\partial w}{\partial r}\right)^2+2\delta\left(u\frac{\partial^2 w}{\partial r\partial z}+w\frac{\partial^2 w}{\partial z^2}\right)\right]. \quad (27)$$

$$\tau_{\theta\theta}=2\delta\frac{u}{r}+2\alpha_1\delta^2\left[\frac{u}{r}\frac{\partial u}{\partial r}-\left(\frac{u}{r}\right)^2+\frac{w}{r}\frac{\partial u}{\partial z}\right]. \quad (28)$$

Where $(\Psi),(\varphi)$ are stream functions of velocity components $u,\ w, u_s$ and w_s that is dimensionless $u=-\frac{1}{r}\frac{\partial\Psi}{\partial z}$, $\frac{1}{r}\frac{\partial\Psi}{\partial r}$,$u_s=-\frac{1}{r}\frac{\partial\varphi}{\partial z}$ and $w_s=\frac{1}{r}\frac{\partial\varphi}{\partial r}$, respectively, and the motion of Equations (20) - (24) becomes:

$$\delta Re\left[\delta^2\left[-\frac{2}{r^2}\frac{\partial\Psi}{\partial z}\frac{\partial^2\Psi}{\partial z^2}+\frac{1}{r}\frac{\partial^3\Psi}{\partial r\partial z^2}\frac{\partial\Psi}{\partial z}-\frac{1}{r}\frac{\partial\Psi}{\partial r}\frac{\partial^3\Psi}{\partial z^3}-\frac{\partial^3\Psi}{\partial z^3}\right]-[-\frac{3}{r^3}\frac{\partial\Psi}{\partial z}\frac{\partial\Psi}{\partial r}-\frac{1}{r^2}\frac{\partial^2\Psi}{\partial z\partial r}\frac{\partial\Psi}{\partial r}+\frac{3}{r^2}\frac{\partial\Psi}{\partial z}\frac{\partial^2\Psi}{\partial r^2}-\frac{1}{r}\frac{\partial\Psi}{\partial z}\frac{\partial^3\Psi}{\partial r^3}+\frac{1}{r}\frac{\partial\Psi}{\partial r}\frac{\partial^3\Psi}{\partial z\partial r^2}-\frac{1}{r}\frac{\partial^2\Psi}{\partial z\partial r}+\frac{\partial^3\Psi}{\partial z\partial r^2}]\right]=\delta\frac{\partial^2}{\partial r\partial z}(r\tau_{rr})+\delta^2 r\frac{\partial^2}{\partial z^2}(\tau_{rz})-\delta\frac{\partial}{\partial z}\tau_{\theta\theta}+\delta^2\left(A-\frac{1}{Da}-H^2\right)\left(\frac{\partial^2\Psi}{\partial z^2}-\frac{\partial^2\varphi}{\partial z^2}\right)-\ r\frac{\partial}{\partial r}(\frac{1}{r}\frac{\partial}{\partial r}(r\tau_{rz}))-\delta r\frac{\partial^2}{\partial z\partial r}(\tau_{zz})-A\left(\frac{\partial^2\varphi}{\partial r^2}-\frac{1}{r}\frac{\partial\varphi}{\partial r}+\frac{1}{r}\frac{\partial\Psi}{\partial r}-\frac{\partial^2\Psi}{\partial r^2}\right)+G_r r\frac{\partial\theta}{\partial r} \quad (29)$$

$$\delta\{\delta^2\left[-\frac{2}{r^2}\frac{\partial\varphi}{\partial z}\frac{\partial^2\varphi}{\partial z^2}+\frac{1}{r}\frac{\partial\varphi}{\partial z}\frac{\partial^3\varphi}{\partial r\partial z^2}-\frac{1}{r}\frac{\partial^3\varphi}{\partial z^3}\frac{\partial\varphi}{\partial r}-\frac{\partial^3\varphi}{\partial z^3}\right]-\left[\frac{-3}{r^3}\frac{\partial\varphi}{\partial r}\frac{\partial\varphi}{\partial z}+\frac{3}{r^2}\frac{\partial^2\partial\varphi}{\partial r^2}\frac{\partial\varphi}{\partial z}-\frac{1}{r}\frac{\partial\varphi}{\partial z}\frac{\partial^3\varphi}{\partial r^3}-\frac{1}{r^2}\frac{\partial\varphi}{\partial r}\frac{\partial^2\varphi}{\partial r\partial z}+\frac{1}{r}\frac{\partial\varphi}{\partial r}\frac{\partial^3\varphi}{\partial r^2\partial z}-\frac{1}{r}\frac{\partial^2\varphi}{\partial r\partial z}+\frac{\partial^3\varphi}{\partial r^2\partial z}\right]\}=B(\delta^2(\frac{\partial^2\varphi}{\partial z^2}-\frac{\partial^2\Psi}{\partial z^2})\ \text{-}\left(\frac{\partial^2\Psi}{\partial r^2}-\frac{1}{r}\frac{\partial\Psi}{\partial r}-\frac{\partial^2\varphi}{\partial r^2}+\frac{1}{r}\frac{\partial\varphi}{\partial r}\right) \quad (30)$$

$$\delta\, Re\, Pr\left[-\frac{1}{r}\frac{\partial\Psi}{\partial z}\frac{\partial\theta}{\partial r}+\left(\frac{1}{r}\frac{\partial\Psi}{\partial r}+1\right)\frac{\partial\theta}{\partial z}\right]=\nabla^2\theta+\beta. \quad (31)$$

From Equation (21) calculate pressure gradient:

$$\frac{dp}{dz}=\frac{1}{r}\frac{\partial}{\partial r}(r\tau_{rz})+\delta\frac{\partial}{\partial z}(\tau_{zz})+\frac{A}{r}\left(\frac{\partial\varphi}{\partial r}-\frac{\partial\Psi}{\partial r}\right)-G_r r\,\theta-\delta Re[-\frac{1}{r}\frac{\partial\Psi}{\partial z}\frac{\partial}{\partial r}\left(\frac{1}{r}\frac{\partial\Psi}{\partial r}\right)+\left(\frac{1}{r}\frac{\partial\Psi}{\partial r}+1\right)\frac{\partial}{\partial z}\left(\frac{1}{r}\frac{\partial\Psi}{\partial r}\right)]. \quad (32)$$

$$\frac{dp}{dr}=0. \quad (33)$$

It is possible to cast the boundary conditions in the dimensionless wave frame:

$$\left.\begin{array}{l}\Psi=0,\ \varphi=0,\ \frac{\partial}{\partial r}\left(\frac{1}{r}\frac{\partial\Psi}{\partial r}\right)=0\,,\frac{\partial\theta}{\partial r}=0\ at\ r=0\\ \Psi=\mathrm{F},\ \varphi=F_s,\ \frac{1}{r}\frac{\partial\Psi}{\partial r}=-1,\theta=0\ \ at\ r=h\end{array}\right\}. \quad (34)$$

5. Approximative analytic solution

To use the perturbation method with help of MATHEMATICA package we can find an approximate analytic solution for the problem under considering. So, let us assume that:

$$\Psi=\ \Psi_0+\delta\Psi_1+\delta^2\Psi_2+o(\delta^3). \quad (35)$$

$$\theta=\theta_0+\delta\theta_1+\delta^2\theta_2+o(\delta^3). \quad (36)$$

$$P=P_0+\delta P_1\,. \quad (37)$$

By substitute the above expression into Equations (35)- (37) and equation the equal power of δ, we obtain the underlying equations of zeroth, first, and second order provided by:

5.1 Zero- order solution of O(δ)

$$-\frac{\partial}{\partial r}\Big(\frac{1}{r}\frac{\partial}{\partial r}\left(r\frac{\partial}{\partial r}\left(\frac{1}{r}\frac{\partial\Psi_0}{\partial r}\right)\right)-A\left(\frac{\partial^2}{\partial r^2}-\frac{1}{r}\frac{\partial}{\partial r}\right)(\varphi_0-\Psi_0)+Gr\,r\frac{\partial\theta_0}{\partial r}=0. \quad (38)$$

$$B\left(\frac{\partial^2}{\partial r^2}-\frac{1}{r}\frac{\partial}{\partial r}\right)(\varphi_0-\Psi_0)=0. \quad (39)$$

$$\left(\frac{\partial^2}{\partial r^2}+\frac{1}{r}\frac{\partial}{\partial r}\right)\theta_0+\beta=0. \quad (40)$$

$$\frac{dP_0}{dz}=\frac{1}{r}\frac{\partial}{\partial r}\left(r\frac{\partial}{\partial r}\left(\frac{1}{r}\frac{\partial\Psi_0}{\partial r}\right)\right)+\frac{A}{r}\frac{\partial}{\partial r}(\varphi_0-\Psi_0)-Gr\,\theta_0. \quad (41)$$

$$\left.\begin{array}{l}\Psi_0=0,\ \varphi_0=0,\ \frac{\partial}{\partial r}\left(\frac{1}{r}\frac{\partial\Psi_0}{\partial r}\right)=0\,,\frac{\partial\theta_0}{\partial r}=0\ at\ r=0\\ \Psi_0=\mathrm{F}_0,\ \varphi_0=F_{s0},\ \frac{1}{r}\frac{\partial\Psi_0}{\partial r}=-1,\theta_0=0\ \ at\ r=h\end{array}\right\}. \quad (42)$$

The solution of the above nonlinear system of (38)- (41) subject to boundary conditions (42), it is found the solution is given by:

$$\theta_0(r,z)=-\frac{1}{4}r^2\beta+c_0. \quad (43)$$

$$\Psi_0(r,z)=\frac{1}{384}r^2(96\left(r^2c_3(z)+2c_1(z)\right)-\beta Gr\,r^4). \quad (44)$$

$$\varphi_0(r,z)=\frac{1}{4}r^4c_3(z)+\frac{1}{2}r^2c_4(z)-\frac{1}{384}\beta Gr\,r^6. \quad (45)$$

$$P_0=-\frac{1}{6144r^2}(-4z(-1536-1536Ar^2+\cdots+3AGrr^2\beta\phi^4)+\cdots-24Ar^2\phi^5\cos(z)\,F_0)), \quad (46)$$

where the constants c_0, c_1, c_3, and c_4 are expressed as:

$c_0=\frac{h^2\beta}{4}$,

$c_1=\frac{4F_0}{h^2}-\frac{1}{192}\ \beta Gr\ h^2+1$,

$c_3=-\frac{2}{h^2}+\frac{1}{48}\ \beta Gr\ h^2-\frac{4F_0}{h^4}$,

$c_4=1-\frac{1}{192}\ \beta Gr\ h^4+\frac{2(F_0+F_{S0})}{h^2}$.

5.2 First- order solution of O(δ)

The first-order approximation of O(δ) fulfills the following equations:

$$Re\left[\frac{3}{r^3}\frac{\partial\Psi_0}{\partial r}\frac{\partial\Psi_0}{\partial z}-\frac{3}{r^2}\frac{\partial^2\Psi_0}{\partial r^2}\frac{\partial\Psi_0}{\partial z}+\frac{1}{r}\frac{\partial^3\Psi_0}{\partial r^3}\frac{\partial\Psi_0}{\partial z}+\frac{3}{r^2}\frac{\partial^2\Psi_0}{\partial r\partial z}\frac{\partial\Psi_0}{\partial r}-\frac{1}{r}\frac{\partial^3\Psi_0}{\partial r^2\partial z}\frac{\partial\Psi_0}{\partial r}+\frac{1}{r}\frac{\partial^2\Psi_0}{\partial r\partial z}-\frac{\partial^3\Psi_0}{\partial r^2\partial z}\right]=$$

$$.\ (47)\ \frac{\partial^2}{\partial r\partial z}(r\tau_{0rr})-r\frac{\partial}{\partial r}\left(\frac{1}{r}\frac{\partial}{\partial r}(r\tau_{1rz})\right)-r\frac{\partial^2}{\partial r\partial z}(\tau_{0zz})-A\left(\frac{\partial^2}{\partial r^2}-\frac{1}{r}\frac{\partial}{\partial r}\right)(\varphi_1-\Psi_1)+Gr\,r\frac{\partial\theta_1}{\partial r}$$

$$\mathrm{B}\Big(\frac{\partial^2}{\partial r^2}-$$

$\frac{\partial^2\varphi_0}{\partial r^2}\Big)(\varphi_1-\Psi_1)=\frac{3}{r^3}\frac{\partial\varphi_0}{\partial r}\frac{\partial\varphi_0}{\partial z}-\frac{3}{r^2}\frac{\partial^2\varphi_0}{\partial r^2}\frac{\partial\varphi_0}{\partial z}+\frac{1}{r}\frac{\partial^3\varphi_0}{\partial r^3}\frac{\partial\varphi_0}{\partial z}+\frac{1}{r^2}\frac{\partial^2\varphi_0}{\partial r\partial z}\frac{\partial\varphi_0}{\partial r}-\frac{1}{r}\frac{\partial^3\varphi_0}{\partial r^2\partial z}\frac{\partial\varphi_0}{\partial r}+\frac{1}{r}\frac{\partial^2\varphi_0}{\partial r\partial z}-\frac{\partial^3\varphi_0}{\partial r^2\partial z}.$ (48)

$\frac{\partial^2\theta_1}{\partial r^2}+\frac{1}{r}\frac{\partial\theta_1}{\partial r}= Re\, Pr\left[-\frac{1}{r}\frac{\partial\Psi_0}{\partial z}\frac{\partial\theta_0}{\partial r}+\frac{1}{r}\frac{\partial\Psi_0}{\partial r}\frac{\partial\theta_0}{\partial z}+\frac{\partial\theta_0}{\partial z}\right].$ (49)

$\frac{dP_1}{dz}=\frac{1}{r}\frac{\partial}{\partial r}(r\tau_{1rz})+\frac{\partial}{\partial z}(\tau_{0zz})+\frac{A}{r}\frac{\partial}{\partial r}(\varphi_1-\Psi_1)-Gr\,\theta_1-Re\left[-\frac{1}{r}\frac{\partial\Psi_0}{\partial r}\frac{\partial}{\partial r}\left(\frac{1}{r}\frac{\partial\Psi_0}{\partial r}\right)+\left(\frac{1}{r}\frac{\partial\Psi_0}{\partial r}+1\right)\frac{\partial}{\partial z}\left(\frac{1}{r}\frac{\partial\Psi_0}{\partial r}\right)\right].$ (50)

Where:

$\tau_{0rr}=\alpha_1[\frac{\partial}{\partial r}\left(\frac{1}{r}\frac{\partial\Psi_0}{\partial r}\right)]^2.$ (51)

$\tau_{1rz}=\frac{\partial}{\partial r}\left(\frac{1}{r}\frac{\partial\Psi_1}{\partial r}\right)+\alpha_1\left[\frac{\partial}{\partial r}\left(\frac{1}{r}\frac{\partial\Psi_0}{\partial r}\right)\frac{1}{r}\frac{\partial^2\Psi_0}{\partial r\partial z}+\frac{\partial}{\partial r}\left(\frac{1}{r}\frac{\partial\Psi_0}{\partial z}\right)\frac{\partial}{\partial r}\left(\frac{1}{r}\frac{\partial\Psi_0}{\partial r}\right)-\frac{1}{r}\frac{\partial\Psi_0}{\partial z}\frac{\partial^2}{\partial r^2}\left(\frac{1}{r}\frac{\partial\Psi_0}{\partial r}\right)+\frac{1}{r}\frac{\partial\Psi_0}{\partial r}\frac{\partial^2}{\partial r\partial z}\left(\frac{1}{r}\frac{\partial\Psi_0}{\partial r}\right)\right].$ (52)

$\tau_{0zz}=-\alpha_1[\frac{\partial}{\partial r}\left(\frac{1}{r}\frac{\partial\Psi_0}{\partial r}\right)]^2.$ (53)

$$\left.\begin{array}{l}\Psi_1=0,\ \varphi_1=0,\ \frac{\partial}{\partial r}\left(\frac{1}{r}\frac{\partial\Psi_1}{\partial r}\right)=0, \frac{\partial\theta_1}{\partial r}=0\ at\ r=0\\ \Psi_1=F_1,\ \varphi_1=F_{s1},\ \frac{1}{r}\frac{\partial\Psi_1}{\partial r}=-1, \theta_1=0\ \ at\ r=h\end{array}\right\}. \quad (54)$$

To solve nonlinear system of Equations (47)- (49), subject to boundary conditions (54), is found in the form of:

$\theta_1=c_6+\frac{1}{221184}Pr\, r^2 Re\beta\phi(\cos(z)(-Gr\beta(144+\cdots+9r^2(4+3\phi^2))+384(72+\cdots+10r^4)\beta)(\sin(2z)))+\frac{Prr^2Re\beta\phi\cos(z)(4r^4+144(1+\phi\sin(z))^4-45(r+r\phi\sin(z))^2)F_o}{288(1+\phi\sin(z))^5}.$ (55)

$\Psi_1=\frac{1}{70778880}(17694720\,(2\,c_7r^2+\ c_9r^4)+\cdots+(1536\,Gr\,Pr\,r^6\,Re\,\beta\,\phi\cos(z)\,(r^4+240\,(1+\phi\,sin(z))^4-25\,(r+r\,\phi\sin(z))^2)\,Fo)/(1+\phi\,sin(z))^5).$ (56)

$\varphi_1(r,z)=\frac{c_9r^4}{4}+\frac{r^2c_{11}}{2}+\cdots+\frac{GrPrr^6Re\beta\phi cos(z)(r^4+240(1+\phi Sin(z))^4-25(r+r\phi sin(z))^2)F_o}{46080(1+\phi sin(z))^5}.$ (57)

$P_1=\frac{-(3623878656r(-3c7+3Ac11r^2-3Ac7r^2+9c9r^2-3c6Grr^2+c7r^3+c9r^5)z(1+\phi Sin(z))^9)}{(-10871635968r^3-195689447424r^3\phi^2+\cdots)}+\cdots+\frac{(-10871635968r^3-195689447424r^3\phi^2-\cdots)}{(-10871635968r^3-195689447424r^3\phi^2+\cdots)}.$

(58)

5.3 Second- order solution of O(δ)

$Re\left[\frac{3}{r^3}\left(\frac{\partial\Psi_0}{\partial r}\frac{\partial\Psi_1}{\partial z}+\frac{\partial\Psi_1}{\partial r}\frac{\partial\Psi_0}{\partial z}\right)-\frac{3}{r^2}\left(\frac{\partial\Psi_0}{\partial z}\frac{\partial^2\Psi_1}{\partial r^2}+\frac{\partial\Psi_1}{\partial z}\frac{\partial^2\Psi_0}{\partial r^2}\right)+\frac{1}{r}\left(\frac{\partial\Psi_0}{\partial z}\frac{\partial^3\Psi_1}{\partial r^3}+\frac{\partial\Psi_1}{\partial z}\frac{\partial^3\Psi_0}{\partial r^3}\right)+\frac{1}{r^2}\left(\frac{\partial\Psi_0}{\partial r}\frac{\partial^2\Psi_1}{\partial r\partial z}+\frac{\partial\Psi_1}{\partial r}\frac{\partial^2\Psi_0}{\partial r\partial z}\right)-\frac{1}{r}\left(\frac{\partial\Psi_0}{\partial r}\frac{\partial^3\Psi_1}{\partial r^2\partial z}+\frac{\partial\Psi_1}{\partial r}\frac{\partial^3\Psi_0}{\partial r^2\partial z}\right)+\frac{1}{r}\frac{\partial^2\Psi_1}{\partial r\partial z}-\frac{\partial^3\Psi_1}{\partial r^2\partial z}\right]=\frac{\partial^2}{\partial r\partial z}(r\tau_{1rr})+r\frac{\partial^2}{\partial z^2}(\tau_{0rz})-\frac{\partial}{\partial z}(\tau_{1\theta\theta})-r\frac{\partial}{\partial r}\left(\frac{1}{r}\frac{\partial}{\partial r}(r\tau_{2rz})\right)-r\frac{\partial^2}{\partial r\partial z}(\tau_{1zz})-A\left(\frac{\partial^2}{\partial r^2}-\frac{1}{r}\frac{\partial}{\partial r}\right)(\varphi_2-\Psi_2)+\left(A-\frac{1}{Da}-H^2\right)\left(\frac{\partial^2\Psi_0}{\partial z^2}-\frac{\partial^2\varphi_0}{\partial z^2}\right)+Gr\,r\frac{\partial\theta_2}{\partial r}.$

(59)

$B\left(\frac{\partial^2\varphi_0}{\partial z^2}-\frac{\partial^2\Psi_0}{\partial z^2}\right)+B\left(\frac{\partial^2}{\partial r^2}-\frac{1}{r}\frac{\partial}{\partial r}\right)(\varphi_2-\Psi_2)=\left[\frac{3}{r^3}\left(\frac{\partial\varphi_0}{\partial r}\frac{\partial\varphi_1}{\partial z}+\frac{\partial\varphi_1}{\partial r}\frac{\partial\varphi_0}{\partial z}\right)-\frac{3}{r^2}\left(\frac{\partial\varphi_0}{\partial z}\frac{\partial^2\varphi_1}{\partial r^2}+\frac{\partial\varphi_1}{\partial z}\frac{\partial^2\varphi_0}{\partial r^2}\right)+\frac{1}{r}\left(\frac{\partial\varphi_0}{\partial z}\frac{\partial^3\varphi_1}{\partial r^3}+\frac{\partial\varphi_1}{\partial z}\frac{\partial^3\varphi_0}{\partial r^3}\right)+\frac{1}{r^2}\left(\frac{\partial\varphi_0}{\partial r}\frac{\partial^2\varphi_1}{\partial r\partial z}+\frac{\partial\varphi_1}{\partial r}\frac{\partial^2\varphi_0}{\partial r\partial z}\right)-\frac{1}{r}\left(\frac{\partial\varphi_0}{\partial r}\frac{\partial^3\varphi_1}{\partial r^2\partial z}+\frac{\partial\varphi_1}{\partial r}\frac{\partial^3\varphi_0}{\partial r^2\partial z}\right)+\frac{1}{r}\frac{\partial^2\varphi_1}{\partial r\partial z}-\frac{\partial^3\varphi_1}{\partial r^2\partial z}\right].$

(60)

$$Re\,\mathrm{Pr}\left[-\frac{1}{r}\left(\frac{\partial\Psi_0}{\partial z}\frac{\partial\theta_1}{\partial r}+\frac{\partial\Psi_1}{\partial z}\frac{\partial\theta_0}{\partial r}\right)+\frac{1}{r}\frac{\partial\Psi_1}{\partial r}+\frac{\partial\theta_1}{\partial z}\right]=\frac{\partial^2\theta_2}{\partial r^2}+\frac{1}{r}\frac{\partial\theta_2}{\partial r}. \quad (61)$$

Where:

$$\tau_{1rr}=-2\frac{\partial}{\partial r}\left(\frac{1}{r}\frac{\partial\Psi_0}{\partial z}\right)+2\alpha_1\frac{\partial}{\partial r}\left(\frac{1}{r}\frac{\partial\Psi_0}{\partial r}\right)\frac{\partial}{\partial r}\left(\frac{1}{r}\frac{\partial\Psi_1}{\partial r}\right). \quad (62)$$

$$\tau_{1\theta\theta}=\frac{-2}{r^2}\frac{\partial\Psi_0}{\partial z}. \quad (63)$$

$$\tau_{1zz}=\frac{2}{r}\frac{\partial^2\Psi_0}{\partial z\partial r}-2\alpha_1\frac{\partial}{\partial r}\left(\frac{1}{r}\frac{\partial\Psi_0}{\partial r}\right)\frac{\partial}{\partial r}\left(\frac{1}{r}\frac{\partial\Psi_1}{\partial r}\right). \quad (64)$$

$$\tau_{2rz}=\frac{\partial}{\partial r}\left(\frac{1}{r}\frac{\partial\Psi_2}{\partial r}\right)-\frac{1}{r}\frac{\partial^2\Psi_0}{\partial z^2}+\alpha_1\Big[\frac{\partial}{\partial r}\left(\frac{1}{r}\frac{\partial\Psi_0}{\partial r}\right)\frac{1}{r}\frac{\partial^2\Psi_1}{\partial r\partial z}+\frac{\partial}{\partial r}\left(\frac{1}{r}\frac{\partial\Psi_1}{\partial r}\right)\frac{1}{r}\frac{\partial^2\Psi_0}{\partial r\partial z}+\frac{\partial}{\partial r}\left(\frac{1}{r}\frac{\partial\Psi_0}{\partial z}\right)\frac{\partial}{\partial r}\left(\frac{1}{r}\frac{\partial\Psi_1}{\partial r}\right)+\frac{\partial}{\partial r}\left(\frac{1}{r}\frac{\partial\Psi_1}{\partial z}\right)\frac{\partial}{\partial r}\left(\frac{1}{r}\frac{\partial\Psi_0}{\partial r}\right)-\frac{1}{r}\frac{\partial\Psi_0}{\partial z}\frac{\partial^2}{\partial r^2}\left(\frac{1}{r}\frac{\partial\Psi_1}{\partial r}\right)-\frac{1}{r}\frac{\partial\Psi_1}{\partial z}\frac{\partial^2}{\partial r^2}\left(\frac{1}{r}\frac{\partial\Psi_0}{\partial r}\right)+\frac{1}{r}\frac{\partial\Psi_0}{\partial r}\frac{\partial^2}{\partial r\partial z}\left(\frac{1}{r}\frac{\partial\Psi_1}{\partial r}\right)+\frac{1}{r}\frac{\partial\Psi_1}{\partial r}\frac{\partial^2}{\partial r\partial z}\left(\frac{1}{r}\frac{\partial\Psi_0}{\partial r}\right)\Big]. \quad (65)$$

$$\left.\begin{array}{l}\Psi_2=0,\ \varphi_2=0,\ \frac{\partial}{\partial r}\left(\frac{1}{r}\frac{\partial\Psi_2}{\partial r}\right)=0, \frac{\partial\theta_2}{\partial r}=0\ at\ r=0\\ \Psi_2=F_2,\ \varphi_2=F_{s2},\ \frac{1}{r}\frac{\partial\Psi_2}{\partial r}=-1, \theta_2=0\ \ at\ r=h\end{array}\right\}. \quad (66)$$

The solution to nonlinear system of Equations (59)- (61) subject to boundary conditions Equation (66), is found in the form of:

$$\theta_2\,(r,z)=\frac{1}{203843174400}((-720\,Gr\,Pr^2\,r^6\,Re^2\,\beta\,\phi\,(-61440+Gr\,\beta\,(8\,r^4+5\,r^2\,(4+3\,\phi^2)+\cdots+\frac{3600\,(1600+Gr\,r^4\,\beta-5\,Gr\,r^2\,\phi\cos(z))\,Fo))}{(1+\phi\sin(z))3}. \quad (67)$$

$$\Psi_2(r,z)=-\frac{5r^4}{64}(\mathrm{A9}+\mathrm{M10}+\mathrm{N9})+\frac{r^6}{192}(\mathrm{A8}+\mathrm{M9}+\mathrm{N8})+\frac{r^7}{525}(\mathrm{A8}+\mathrm{M9}+\mathrm{N7})+\frac{r^8}{1152}(\mathrm{A7}+\mathrm{M9}+\mathrm{N6})+\frac{r^9}{2205}(\mathrm{A6}+\mathrm{M8}+\mathrm{N5})+\frac{r^{10}}{3840}(A5+M8+N4)+\frac{r^{11}}{6237}(A4+M7+N3)+\frac{r^{12}}{9600}(A3+M6+N2)+\frac{r^{13}}{14157}(A2+M5)+\frac{r^{14}}{20160}(A1+M4+N1)+\frac{\mathrm{M3}r^{15}}{27885}+\frac{\mathrm{M2}r^{16}}{37632}+\frac{\mathrm{M1}r^{17}}{49725}-\frac{5r^4\mathrm{S1}}{64}+(\frac{1}{\mathrm{Da}}+H^2)(\frac{r^8\mathrm{S2}}{6144}-\frac{r^6\mathrm{S4}}{384}+\frac{r^6\mathrm{S5}}{384})+\frac{r^6\mathrm{S3}}{192}+\frac{r^2\mathrm{u1}}{2}+\frac{r^4\mathrm{u3}}{4}+\frac{1}{16}r^4\mathrm{Log}[r](A9+M10+N9+S1). \quad (68)$$

Where coefficients $c_6, c_7, c_9, \mathrm{c}_{11}, A1, A2, \ldots, A9$, $M1, M2, \ldots, M10$, $N1, N2, \ldots, N9$, $S1, S2, \ldots, S5, u1, u2$ are constant numbers.

6. Results and discussion

The analysis of "θ" temperature, "u", "w" axial velocity, "P" pressure and "Ψ" stream function is determined in this section.

6.1 The Distribution of temperature

Graphic results present how the parameters contributing to the temperature behave. Figure (2) illustrates how various values of $\beta, Gr, Pr, Re, \delta$ and $\emptyset$ effect the temperature. According to the figures, the temperature distribution behaves in a parabolic manner. In Figures (a) and (b) of Figure (2), we observed an increase in temperature with increasing values of β and Gr, respectively. The increase in temperature at the start and end of the channel is little, and it is increasing in the center of it. In Figures (c), (d), (e) and (f) of Figure (2) we observed a decrease in temperature with an increase in values of $, Pr, Re, \delta$ and $\emptyset$. The decrease in temperature at the start and end of the channel is little, and it is increasing in the center of it.

6.2 The Distribution of velocity

The results of the simulated experiments show the behavior of parameters graphically, where u represents the velocity on the axis of flow. The outcomes of using different values of β, $Gr, Pr, Re, \delta, Da, H, \emptyset,$ and α_1 on the axial velocity u and w are presented in Figures (3) and (4), respectively, so we can see the velocity distribution has a parabolic behavior. In Figures (a) and (d) of Figure (3), observed that the velocity decreases in the middle and at one wall of the boundary channel and not change or little at the other as β and Re increases. According to Figure (e) of Figure (3), phase difference δ is shown to reduce in the middle of the channel while it rises at one wall boundary and lowers at the other. In Figures (f), (h) and (g) of Figure (3) it is observed that the completely opposite effect on velocity with change in parameters H (Hartman number), $\emptyset$ (the ratio between wave amplitude and radius of channel) and Da (Darcy number), these figures cleared that the velocity increases as H and $\emptyset$ increases whereas increases in Da reduce the velocity. In figure (i) of figure (3) the velocity profile u merges in the left of channel's boundary and decreases in the center and in the right of it as α_1 increases. In Figure (a) of Figure (4) observed that the increase in w in the left of channel is little and decreases in the center and in the right of it with increase of the β. It observed from Figure (b) of Figure (4) the velocity w increases in the left and decreases in the center and right of the channel with increase of the Gr. It observed from the Figures (c), (d), (e), (g) , (h) and (i) of the Figure (4) that, the velocity w increases with increase in Re, Pr, δ, Da , $\emptyset$ and α_1. In Figure (f) of the Figure (4) observed that, the velocity decreases in the intervals $0 \le r \le 0.5$, $1 < r$, and increases in the interval $0.5 \le r \le 1$ with increase in H.

6.3 The distribution of pressure

The behavior of the pressure profile for different value of β, $Gr, Pr, Re, \delta, \emptyset,$ and α_1 can be shown in Figure (5). In Figures (a), (b), (e), (f) and (g) of Figure (5), observed that the pressure increases with increase in β, Gr while it decreases with increase in $\delta, \emptyset,$ and α_1. The pressure decreases for $z \in [-2.5, -2]$ and it increases for $z \in [-1, -0.5]$ with increase in Pr in figure (c) of figure (5). In Figure (d) of Figure (5), the pressure decreases for $z \in [-2.5, -1.5]$ and it increases for $z \in [-1, -0.5]$.

6.4 Trapping phenomenon

This section is allocated to discuss the effect of various values β, $Gr, Pr, Re, \delta, Da, H, \emptyset,$ and α_1 on the stream function. Contour graphs present the fluid's flow pattern. Figures (6 –14), show the streamline patterns of fluid under the effect of the different above parameters. In Figures (6 – 8), it was observed that the volume of the bolus increases with increasing values of β, $Gr, Pr,$ respectively. In Figures (9-11) and Figure 13, it is noticed that the number of the bolus reduces and size of it increase with the increase in the value of Re, δ, H and $\emptyset$. In Figure (12), it was observed that the effect of Darcy number (Da) is very small, as the bolus size decreases by a small percentage with an increase in the Darcy number. Also, it was noticed that increasing the values of α_1 leads to increase in the bolus size in Figure 14.

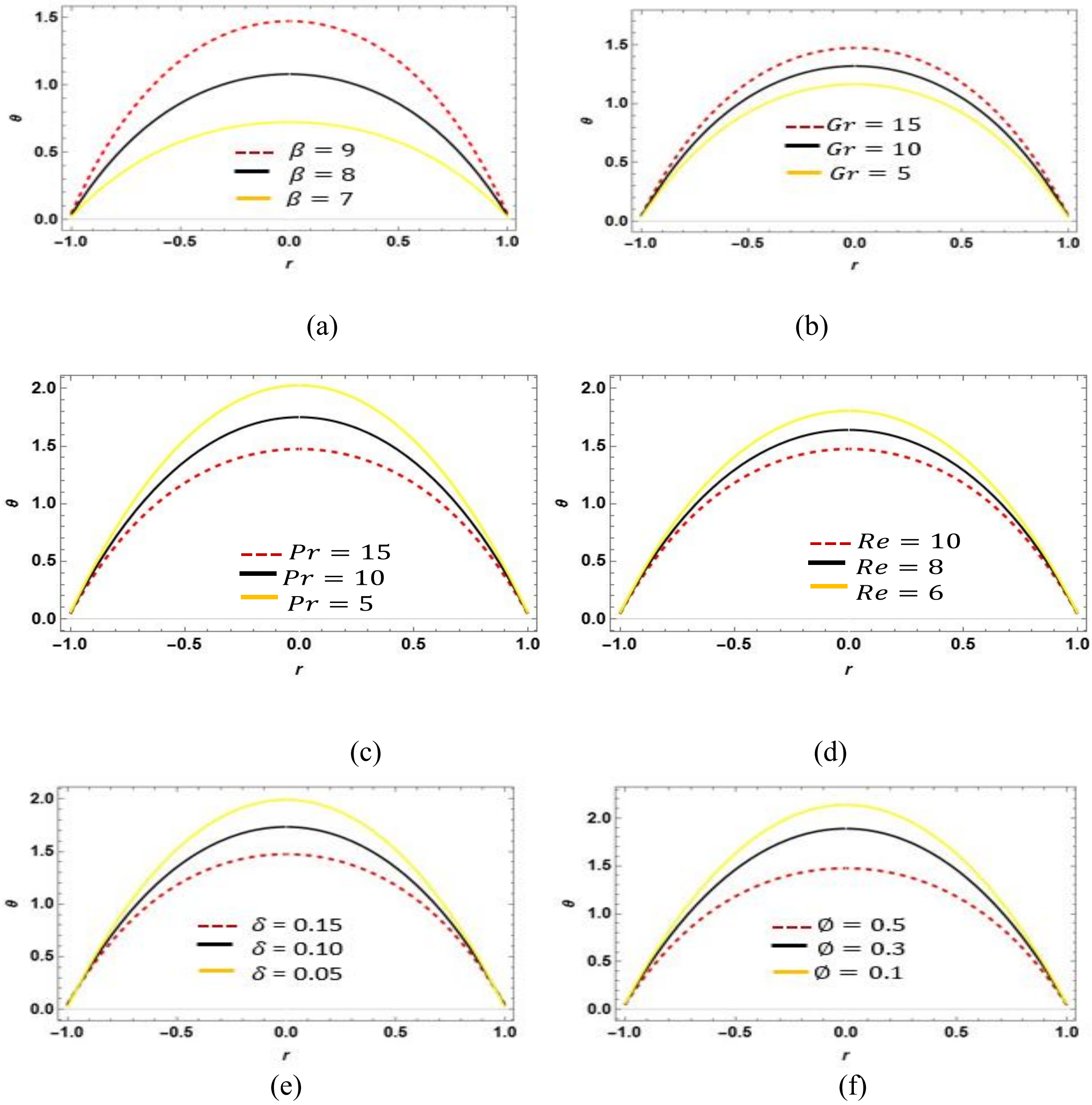

Figure 2: The different values of $\beta, Gr, Pr, Re, \delta$ and $\emptyset$ for variation of temperature θ.

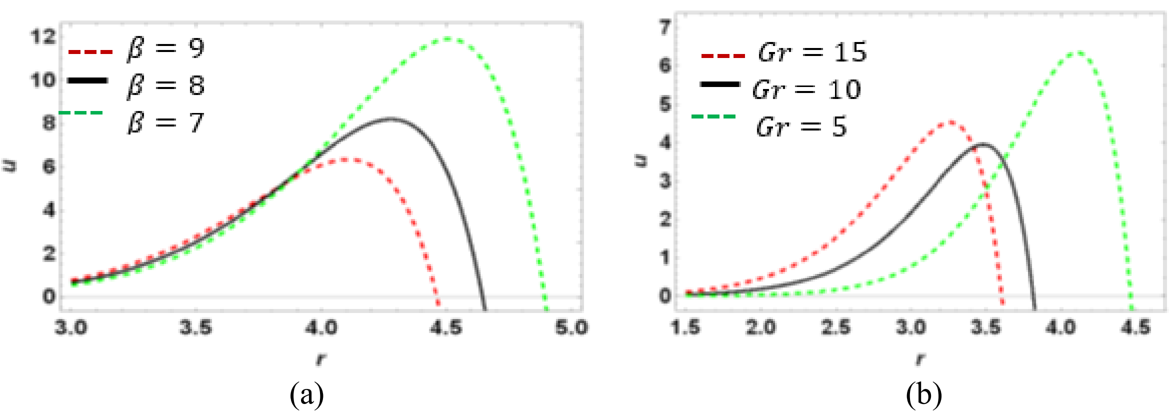

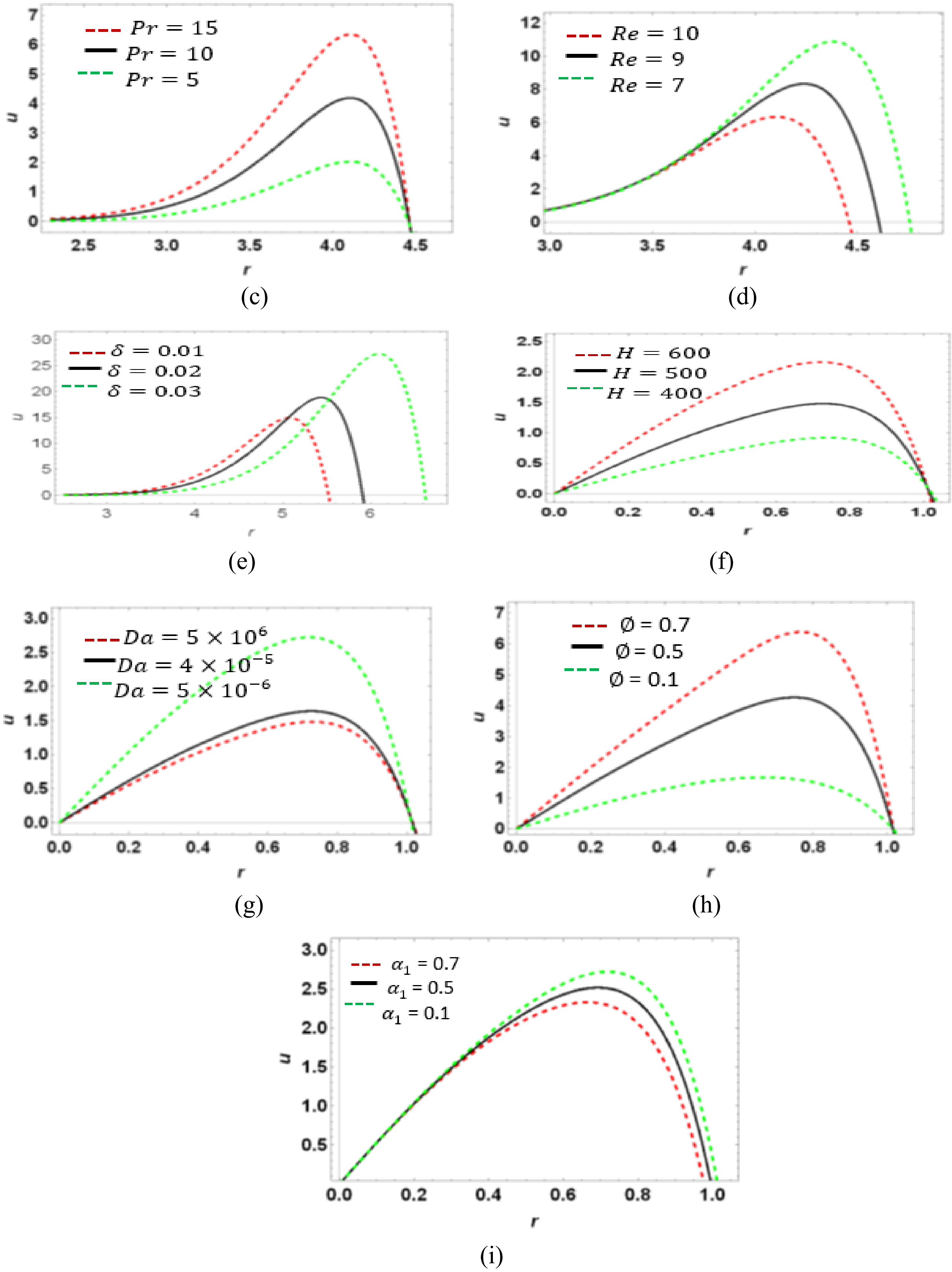

Figure 3: The different values of $\beta, Gr, Pr, Re, \delta, \emptyset, \alpha_1, H, Da$ for variation of velocity u.

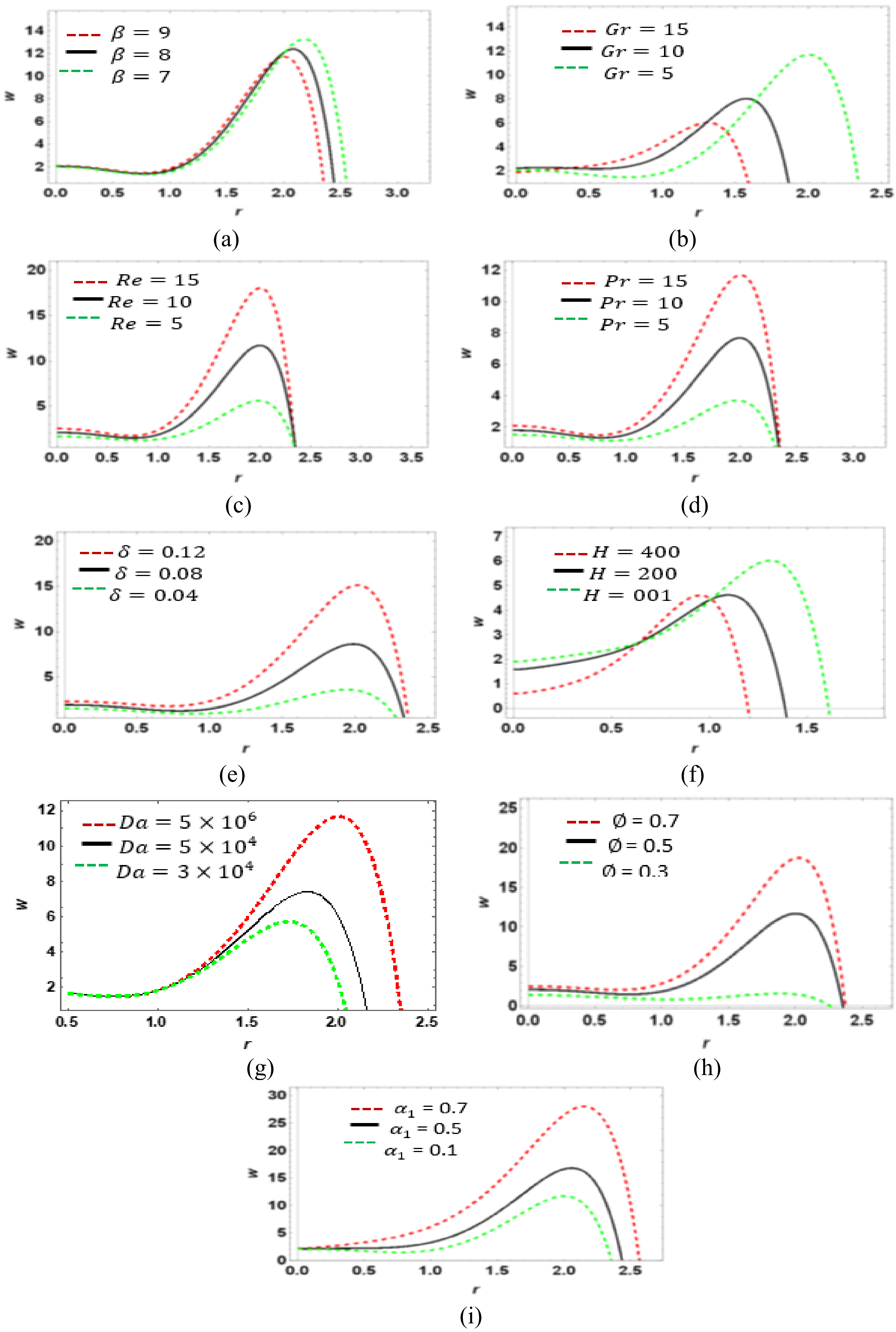

Figure 4: The different values of $\beta, Gr, Pr, Re, \delta, \emptyset, \alpha, H, Da$ for variation of velocity w.

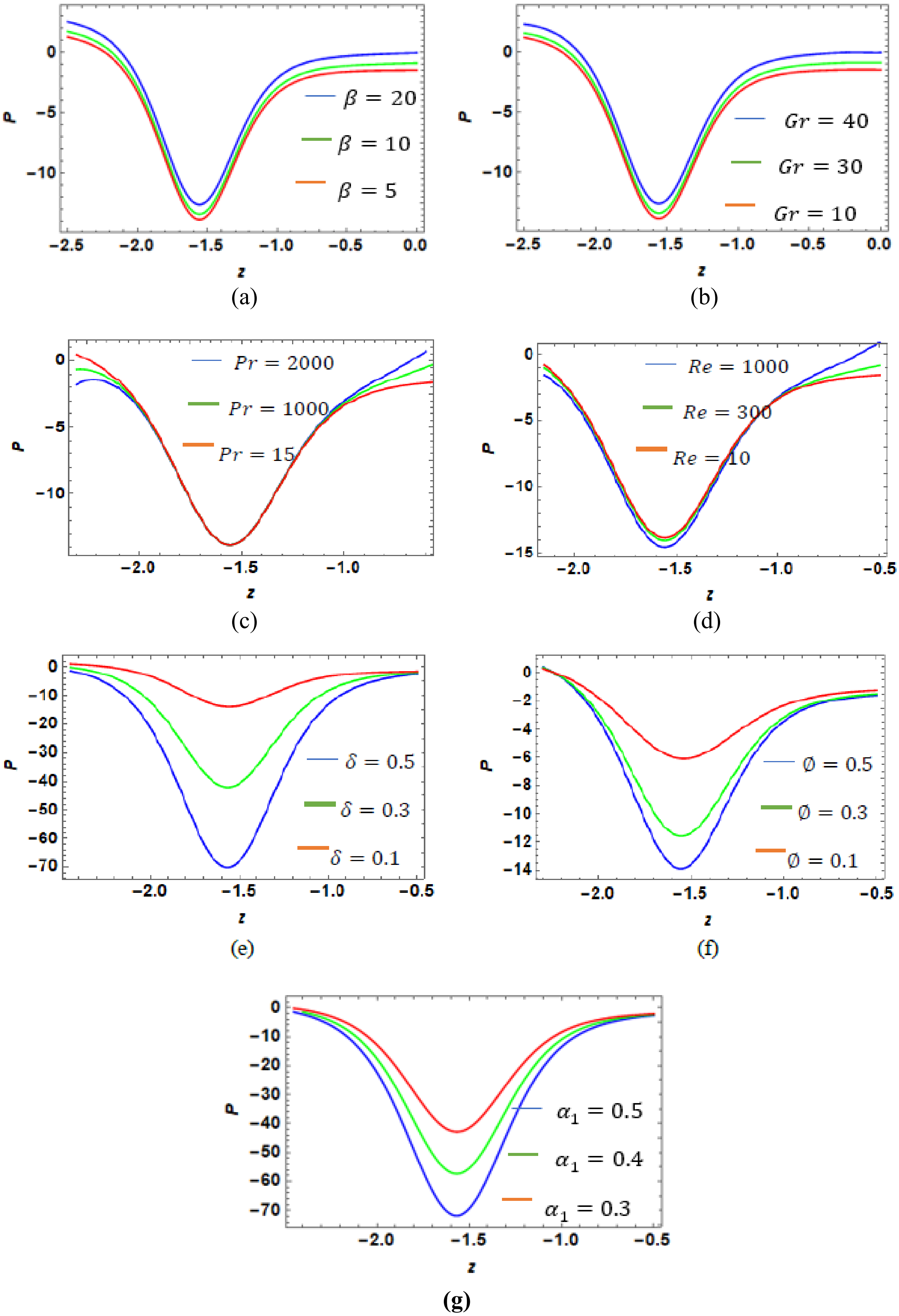

Figure 5: The different values of $\beta, Gr, Pr, Re, \delta, \emptyset$ and α for variation of pressure P.

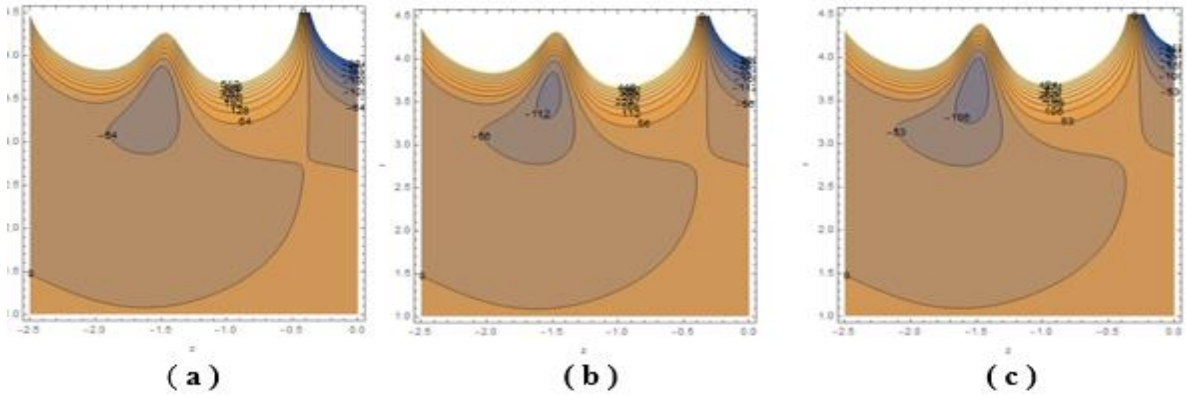

Figure 6: $Gr = 5, Pr = 15, Re = 1, \delta = 0.1, H = 1, \ Da = 10, \ \phi = 0.5, \alpha_1 = 0.1$ $\big((a)\beta = 9, (b)\beta = 8, (c)\beta = 7\big)$.

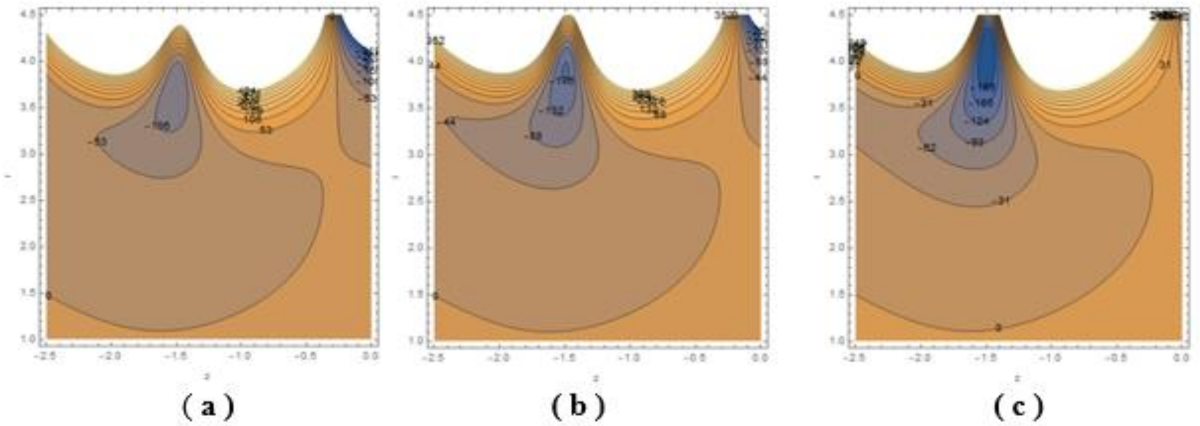

Figure 7:$\beta = 7, \ Pr = 15, Re = 1, \delta = 0.1, H = 1, \ Da = 10, \phi = 0.5, \alpha_1 = 0.1 \ \big((a)Gr = 5, (b)Gr = 4, (c)Gr = 3\big)$.

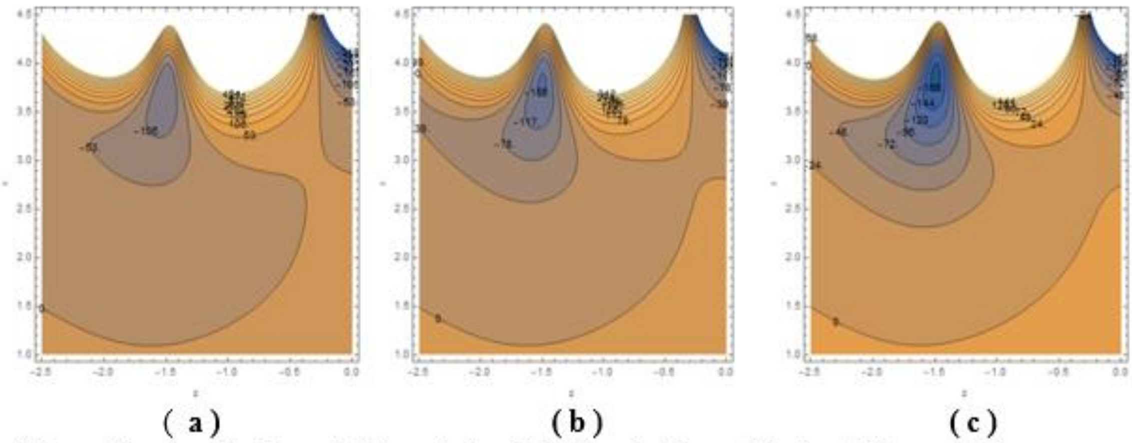

Figure 8: $\beta = 7$:, $Gr = 5, Re = 1, \delta = 0.1, H = 1, \ Da = 10, \phi = 0.5, \alpha_1 = 0.1$ $\big((a)Pr = 15, (b)Pr = 10, (c)Pr = 5\big)$.

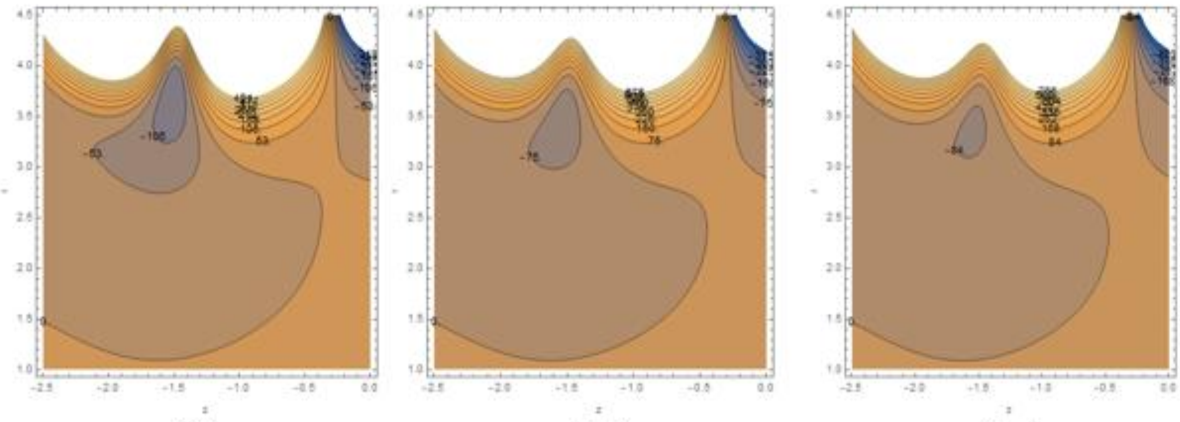

(a) (b) (c)

Figure 9: $Pr = 15,\ \beta = 7, Gr = 5, \delta = 0.1,\ H = 1, Da = 10, \phi = 0.5, \alpha = 0.1$
$(a)Re = 1, (b)Re = 1.2, (c)\ Re = 1.3)$.

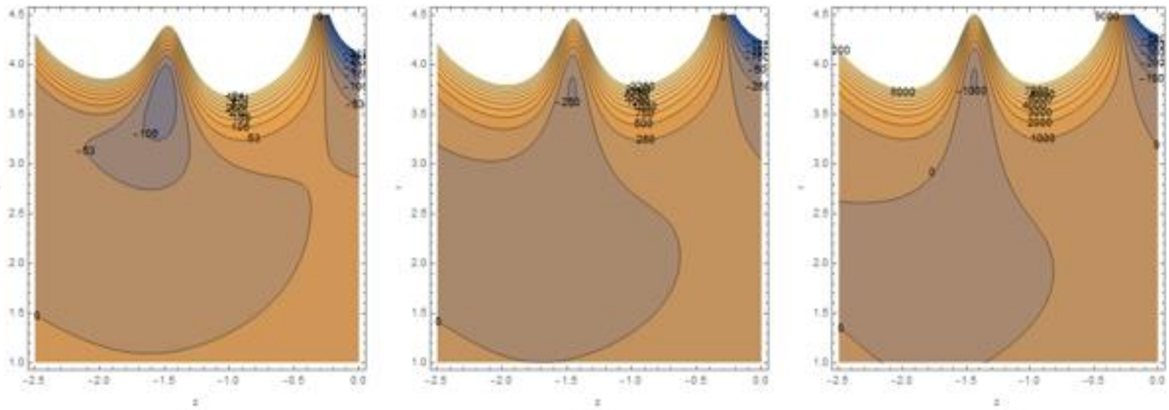

(a) (b) (c)

Figure 10:, $Re = 1, Pr = 15, \beta = 7, Gr = 5, H = 1,\ Da = 10, \phi = 0.5, \alpha = 0.1$
$\left((a)\delta = 0.1, (b)\delta = 0.2, (c)\delta = 0.3\right)$.

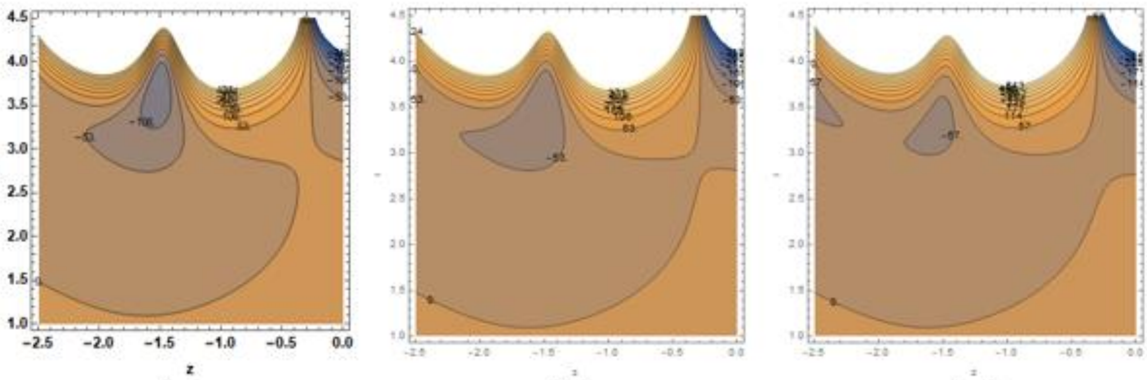

(a) (b) (c)

Figure 11: $\delta = 0.1, Re = 1, Pr = 15, \beta = 7, Gr = 5,\ Da = 10, \phi = 0.5, \alpha_1 = 0.1$
$\left((a)H = 1, (b)H = 5, (c)H = 7\right)$.

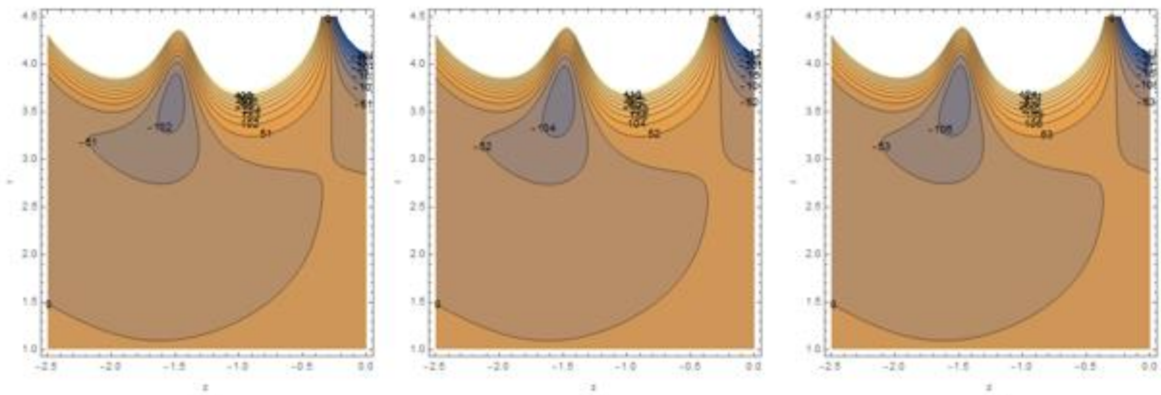

(a) (b) (c)

Figure 12: $H = 1, \delta = 0.1, Re = 1, Pr = 15, \beta = 7, Gr = 5, \phi = 0.5, \alpha_1 = 0.1$
$((a)Da = 0.1, (b)Da = 0.5, (c)Da = 1)$

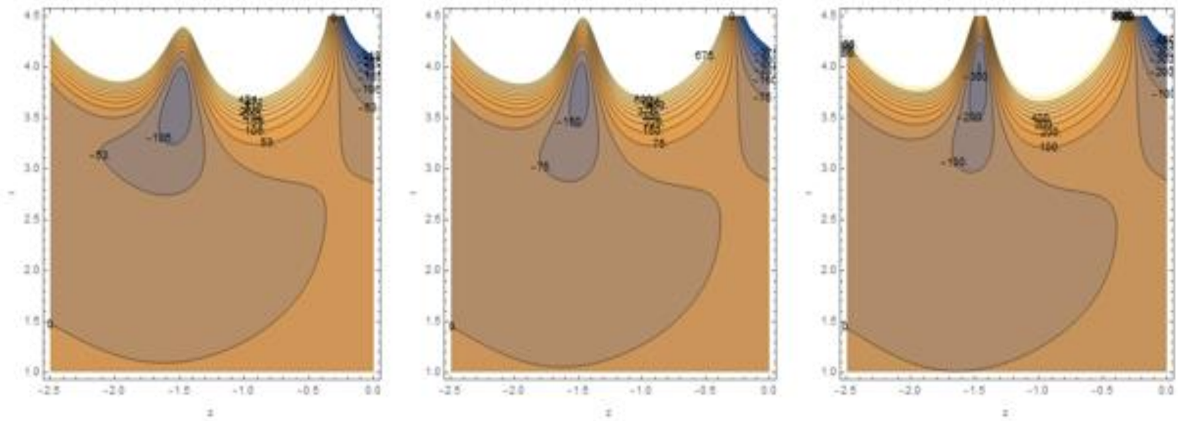

(a) (b) (c)

Figure 13: $Da = 10, H = 1, \delta = 0.1, Re = 1, Pr = 15, \beta = 7, Gr = 5, \alpha_1 = 0.1$
$((a)\phi = 0.52, (b)\phi = 0.53, (c)\phi = 0.54)$.

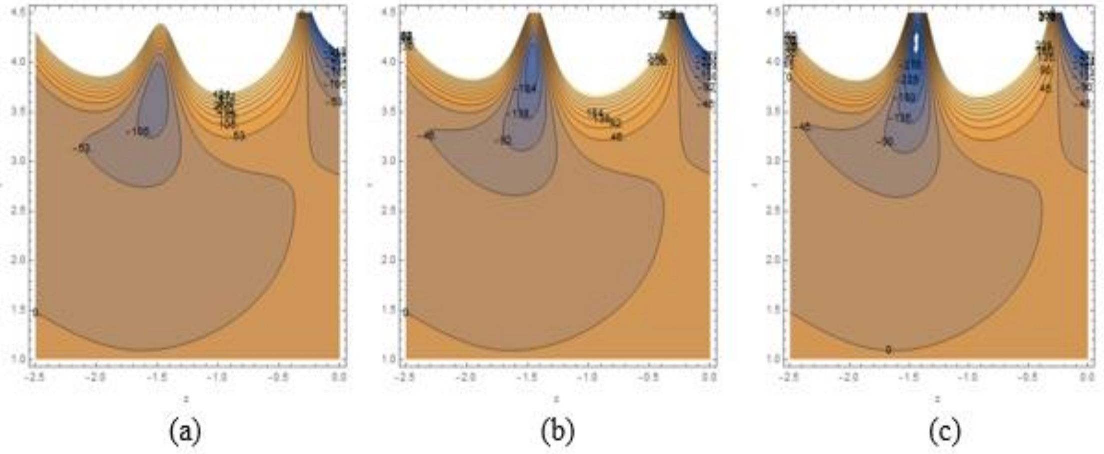

Figure 14: $\phi = 0.5, Da = 10, H = 1, \delta = 0.1, \ Re = 1, Pr = 15, \beta = 7, Gr = 5$
$((a)\alpha_1 = 0.12, (b)\alpha_1 = 0.13, (c)\alpha_1 = 0.15)$

7. Conclusions

The peristaltic transport of a second-grade dusty fluid through a symmetric channel in the porous media and magnetic field under the effect of the physical parameters is studied in this paper. We obtained approximate analytic solution of our problem, and the results are as follows:

1. The temperature increase at the start and end of the channel is little, and it is increasing in the center of it with increasing values of β and Gr. However, opposite with an increase in Pr, Re, δ and $\emptyset$.
2. The effect of increasing the permeability of the porous medium on the size and number of boluses is very small, as the bolus size decreases by a small percentage with an increase in the Darcy number.
3. The velocity profile u decreases with an increase in the permeability of the porous medium (Darcy number) while it increases with increase in Hartman number.
4. The velocity profile w decreases with an increase in Hartman number while it increases with increase in permeability of the porous medium (Darcy number).
5. The pressure increases with increase in β, Gr while it decreases with increase in $\delta, \emptyset,$ and α_1. The pressure decreases for $z \in [-2.5, -2]$ and it increases for $z \in [-1, -0.5]$ with increase in Pr.
6. We observed that the number of the bolus reduces and size of it increase with the increase in the value of Hartman number.

Reference

[1] Noor AL-Huda Kareem AL-Khalidi; Dheia G. Salih Al-Khafajy "Motion, temperature, and concentration analysis of the MHD peristaltic flow of Jeffrey fluid through an endoscopic hollow flexible duct," in *AIP Conference Proceedings*, vol. 3009, no. 1: AIP Publishin, 2024.

[2] Samah F. Jaber AL-khulaifawi and Dheia G. Salih Al-Khafajy, "MHD Peristaltic Flow of a Couple-Stress with varying Temperature for Jeffrey Fluid through Porous Medium," in *Journal of Physics: Conference Series*, vol. 1591, no. 1: IOP Publishing, p. 012075, 2020.

[3] A. Amer and M. A. Murad, "The influence of heat transfer on peristaltic transport of MHD viscoplastic fluid with variable viscosity through symmetric porous channel," in *AIP Conference Proceedings*, vol. 2834, no. 1: AIP Publishing, 2023.

[4] F. Bayones, A. Abd-Alla, and E. N. J. C. Thabet, "Effect of heat and mass transfer and magnetic field on peristaltic flow of a fractional Maxwell fluid in a tube," *Hindawi Complexity*, vol. 2021, pp. 1-12, 2021.

[5] M. O. Kadhim and L. Z. Hummady, "Effect of the Magnetic Field and Rotation on Peristaltic Flow of A Bingham Fluid in Asymmetric Channel with Porous Medium," *Iraqi Journal of Science,* vol. 65, no. 3, pp. 1578-1590, 2024.

[6] Dongsheng Li, Kun Li, Haibin Li, "Oscillating flow of Jeffreys fluids in a semicircular channel," *Chinese Journal of Physics,* vol. 84, pp. 414-428, 2023.

[7] A. M. Nassief and A. M. Abdulhadi, "Rotation and magnetic force effects on peristaltic transport of non-newtonian fluid in a symmetric channel," *Ibn AL-Haitham Journal For Pure and Applied Sciences,* vol ,36 .no. 2, pp. 436-453, 2023.

[8] M. Rashid, K. Ansar , S. Nadeem "Effects of induced magnetic field for peristaltic flow of Williamson fluid in a curved channel" *Journal of Physica A: Statistical Mechanics and its Applications*, vol. 553, pp. 123979, 2020.

[9] H. Vaidya, O. D. Makinde, R. Choudhari, K. V. Prasad, S. U. Khan, and K. Vajravelu, "Peristaltic flow of non-Newtonian fluid through an inclined complaint nonlinear tube: application to chyme transport in the gastrointestinal tract," *The European Physical Journal Plus,* vol. 135 ,no. 11, pp. 1-15, 2020.

[10] F. Ali, A. Zaib, M. Abbas, G. Anitha, K. Loganathan, and G. R. Reddy, "Radiative flow of cross ternary hybrid nanofluid (MoS2, TiO2, Ag/CMC-water) in a Darcy Forchheimer porous medium over a stretching cylinder with entropy minimization," *Heliyon,* vol.10, pp.18 2024*.*

[11] A. M. Siddiqui and W. H. Schwarz, "Peristaltic flow of a second-order fluid in tubes," *Journal of Non-Newtonian Fluid Mechanics,* vol. 53, pp. 257-284, 1994.

[12] T. Salahuddin, A. Arif, A. Haider, and M. Malik, "Variable fluid properties of a second-grade fluid using two different temperature-dependent viscosity models," *Journal of the Brazilian Society of Mechanical Sciences and Engineering,* vol. 40, pp. 1-9, 2018.

[13] H. Tariq and A. Khan, "Peristaltic transport of a second-grade dusty fluid in a tube," *Journal of Mechanical Engineering,* vol. 11, no. 2, pp. 11-25, 2020.

[14] AM Abd-Alla, SM Abo-Dahab, RD El-Semiry, "Long wavelength peristaltic flow in a tubes with an endoscope subjected to magnetic field" *Korea-Australia Rheology Journal,* vol. 25, pp. 107-118, 2013.

[15] N. T. El-dabe, G. M. Moatimid, M. Hassan, M. Mostapha, and T. Physics, "Electrohydrodynamic peristaltic flow of a viscoelastic Oldroyd fluid with a mild stenosis: application of an endoscope" *Journal of Applied Mechanics and Technical Physics,* vol. 57, pp. 38-54, 2016.

[16] Noha M. Hafez, R. D. Alsemiry, S. A. Alharbi, and A. J. S. R. Abd-Alla, "Peristaltic transport characteristics of a second-grade dusty fluid flown with heat transfer through a tube revisited," *Journal of Scientific Reports* vol. 12, no. 1, p. 21605, 2022.

[17] M. Hameed, A.A. Khan, R. Ellahi, M. Raza, "Study of magnetic and heat transfer on the peristaltic transport of a fractional second grade fluid in a vertical tube," *Engineering Science and Technology, an International Journal*, vol. 18, no. 3, pp. 496-502, 2015.

[18] T. Hayat, H. Zahir, A. Tanveer, A. Alsaedi, "Numerical study for MHD peristaltic flow in a rotating frame," *Journal of Computers in Biology and Medicine,* vol. 79, pp. 215-221, 2016.

[19] M. V. Krishna, B. Swarnalathamma, A Chamkha, and Science, "Investigations of Soret, Joule and Hall effects on MHD rotating mixed convective flow past an infinite vertical porous plate" *Journal of Ocean Engineering and Science,* vol. 4, no. 3, pp. 263-275, 2019.

[20] K. Ramesh and M. Devakar, "Effect of heat transfer on the peristaltic transport of a MHD second grade fluid through a porous medium in an inclined asymmetric channel" *Chinese Journal of Physics,* vol. 55, no. 3, pp. 825-844, 2017.

[21] M. S. Reddy, M.V. Reddy, B. J. Reddy, S.R. Krishna, "Peristaltic pumping of Jeffrey fluid with variable viscosity in a tube under the effect of magnetic field", *Journal of Mathematical and Computational Science,* vol. 2, no. 4, pp.2012 ,925-907 .

[22] T. Hayat, M. Rafiq, A. Alsaedi, and B. Ahmad, "Radiative and Joule heating effects on peristaltic transport of dusty fluid in a channel with wall properties," *The European Physical Journal - Plus,*vol. 129, pp. 1-17, 2014.

[23] M. Gnaneswara Reddy" ,Heat and mass transfer on magnetohydrodynamic peristaltic flow in a porous medium with partial slip," *Alexandria Engineering Journal,* vol. 55, no. 2, pp. 1225-1234, 2016.

[24] A. Abd-Alla, S. Abo-Dahab, M .Elsagheer, "Influence of magnetic field and heat and mass transfer on the peristaltic flow through a porous rotating medium with compliant walls," *Journal of Multidiscipline Modeling in Materials and Structures,* vol. 13, no. 4, pp. 648-663, 2017.

[25] A. Bahmani and Hadi Kargarsharifabad, "Laminar natural convection of power-law fluids over a horizontal heated flat plate," *Wiley's Journal,* **,** vol. 48, no. 3, pp. 1044-1066, 2019.

[26] A. Magesh and M. Kothandapani, "Heat and mass transfer analysis on non-Newtonian fluid motion driven by peristaltic pumping in an asymmetric curved channel," *The European Physical Journal Special Topics,* vol. 230, no ,5 .pp. 1447-1464, 2021.

[27] C. Estebe *et al.*, "A low mach number, adaptive mesh method for simulating multi-phase flows in cryogenic fuel tanks," in *Proceedings of the SIAM Conference on Computational Science and Engineering, Philadelphia, PA, US* , vol. 25, 2021 .

[28] A. Moradikazerouni, M. Vahab, and K. Shoele, "A multinode-CFD simulation of a cylindrical pressurized cryogenic storage tank," in *AIAA AVIATION FORUM*, vol. 2021, 2021.

[29] J. E. Dunn and R. L. Fosdick, "Thermodynamics, stability, and boundedness of fluids of complexity 2 and fluids of second grade," *Archive for Rational mechanics and Analysis,* vol. 56, pp. 191-252, 1974.

[30] A. Siddiqui and W. Schwarz, "Peristaltic flow of a second-order fluid in tubes," *Journal of Non-Newtonian Fluid Mechanics,* vol. 53, pp. 257-284, 1994.